Fusion of Weigh-in-Motion System and Bridge Monitoring Data for Bridge Load Rating

Rui Hou[1], Yash Amit Dedhia[1], Seongwoon Jeong[2], Kincho Law[2], Mohammed Ettouney[3], Jerome P. Lynch[1]

[1] *University of Michigan, Ann Arbor, Michigan, USA, Email: jerlynch@umich.edu*

[2] *Stanford University, Stanford, CA, USA*

[3] *Mohammed Ettouney LLC, West New York, New Jersey, USA*

Abstract

Bridge load rating is an important approach to assessing the load-carrying capacity of bridges. Current approaches rely on empirically fitted models that do not require the measurement of live loads and bridge responses; this can lead to rating factors that are conservative. More accurate and bridge-specific load rating methods could be valuable in managing the safety of bridges. In this study, a data-driven load rating approach is proposed based on data collected from a highway corridor with bridge monitoring systems, traffic cameras and weigh-in-motion (WIM) stations linked together in a cohesive cyber-physical system (CPS) architecture. The CPS architecture is designed to capture and track trucks in the corridor so that bridge excitations can be attributed to measured truck weight parameters. Computer vision algorithms, namely convolutional neural networks, are embedded with traffic cameras to automate the identification of trucks using edge computing. This allows bridge responses to a given truck to be conclusively linked to truck weight parameters measured by a WIM station that is not collocated with the bridge. Based on truck weight and bridge strain response data, essential load rating parameters such as the dynamic load allowance are estimated and investigated under various loading scenarios. This can lead to more accurate load ratings specific to the monitored bridge. The I-275 north bound corridor between Newport, Michigan and Romulus, Michigan is instrumented as a testbed to validate the proposed data-drive load rating framework.

1. Introduction

Bridges require proper inspection and assessment to ensure they operate safely. Bridges are inspected regularly to confirm the bridge condition is safe and the bridge system is operating as designed. For safe operations, the load demand imposed on bridge components must be below the structural capacity of those components. Bridge load rating provides a rational basis for assessing the safe load capacity of a bridge. Current load rating methods in the United States follow the Manual for Bridge Evaluation (MBE) published by American Association of State Highway and Transportation Officials (AASHTO); the MBE provides a framework for assessing the bridge capacity based on existing structural conditions, material properties, and loading scenarios, among other considerations (AASHTO 2018). Two load rating methods are recommended by the MBE: analytical and empirical. The analytical method is based on a mechanics-based model but is known

to be unnecessarily conservative due to the use of simplifying assumption (*e.g*. line girder analysis) and model calibration parameters empirically derived that neglect the systematic behavior of the specific bridge being analyzed (Sanayei et al. 2015). The empirical method is based on *in situ* load testing where controlled loads are placed on the bridge and the bridge response is measured. Load testing allows for proper adjustment of the rating factor obtained from the analytical method. The analytical method is most common due to the high costs and logistical complexities (*e.g*., road closure) associated with load testing.

New approaches to bridge load rating are being explored using finite element method (FEM) modeling and structural monitoring. For example, bridge load rating using a calibrated FEM model has been studied with FEM models better reflecting the systematic behavior of a bridge as compared to the simplistic modeling approach taken in the MBE analytical approach (Alipour et al. 2016; Bell et al. 2013; Deng and Phares 2016; Ndong et al. 2019; Sanayei et al. 2015). These methods are even more accurate when the FEM model is calibrated using either modal properties extracted from: bridge vibration measurements (Alipour et al. 2016; Ndong et al. 2019) or strain measurements during controlled truck loading (Bell et al. 2013; Deng and Phares 2016; Sanayei et al. 2015). An alternative approach is to measure bridge responses to heavy trucks whose trajectories on the bridges are tracked using cameras; assuming the bridges is a linear system, the unit influence line (UIL) can be estimated using measured strain responses (Catbas et al. 2012). A limitation of such an approach is the uncertainties associated with estimating vehicle axle spacing and weights, leading to uncertainty in the final rating factor. Finally, some researchers have explored the use of long-term monitoring data to extract maximum bridge strain responses under the actual bridge traffic for use within the analytical MBE model (Al-Khateeb et al. 2018). A challenge of this approach is that the truck loads are not measured and hence, there is no basis for comparing the observed loads with design loads. This makes the rating factors difficult to be compared with those using classical design loads.

The goal of this study is to develop a data-driven load rating method consistent with the MBE analytical approach based on measured bridge responses corresponding to known (measured) truck loads. Specifically, the study shows that it is feasible to link measured bridge responses to truck axle weights measured using a weigh-in-motion (WIM) station by identifying the truck through computer vision. A cyber-physical system (CPS) framework is proposed that collects the data from bridge monitoring systems, cameras and WIM stations, and uses the data collected to link bridge responses to truck measurements. Over time, an abundance of coupled vehicle load and bridge response data can be collected from which load rating parameters can be extracted including the dynamic load allowance (DLA) and UILs. By doing so, the final rating factors from the MBE analytical method reflect the true behavior of the bridge under real load conditions leading to a more accurate assessment of the bridge load capacity. The CPS architecture has been installed on a 20-mile segment of the north-bound I-275 corridor between Newport and Romulus, Michigan which includes two instrumented bridges and a WIMS station. In this paper, the three interior girders of the Newburg Road Bridge are rated following the Load and Resistance Factor Rating (LRFR) criteria for design load rating (AASHTO 2018). To evaluate the proposed data-driven load rating method, the rating factors obtained by the data-driven method are compared with those obtained by conventional analytical and FEM-based methods.

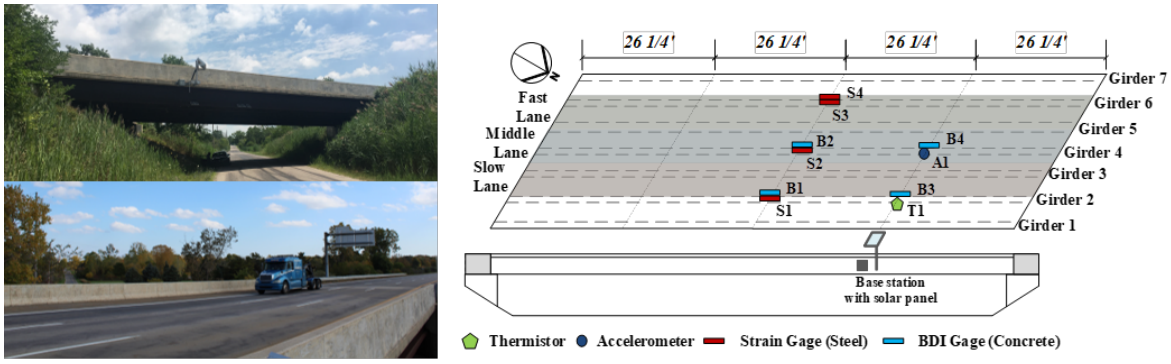

(a) (b)

Figure 1. (a) Views of the Newburg Road Bridge; (b) instrumentation design of the Newburg Road Bridge monitoring system.

2. Corridor-based Cyber-Physical System

2.1 Newburg Road Bridge

The Newburg Road Bridge (NRB) is a single-span composite slab-on-steel girder bridge that carries I-275 north bound traffic over the East Newburg Road in Monroe, Michigan (*Figure 1(a)*). The bridge was built in 1973 and is owned by the Michigan Department of Transportation (MDOT). It spans 105 feet (32.00 m) and has a skew angle of 59 degrees. The bridge consists of seven girder lines (deep I-beam sections). Based on prior inspection, the bridge structural components (*e.g.*, deck, girders, abutments) are generally rated in good condition. For the purpose of long-term SHM, three interior girders (girder lines 2, 4 and 6 in *Figure 1b*) were instrumented with *Narada* wireless sensor nodes measuring bridge strain and acceleration in 2016 (Hou et al. 2017); the sensor layout is depicted in *Figure 1(b)*. A total of 10 sensors are installed including one vertical accelerometer, one thermometer, four weldable strain gages, and four BDI transducers (full bridge strain sensors). In this study, the sensors used for load rating are the weldable strain gages (Hitec HBWF-35-125-6-10GP-TR) placed 3 inches (7.62 cm) above the bottom flange on the I-section web. These strain sensors measure the flexural strain response of the span on girder line 2, 4 and 6 at sensor S1, S2 and S3, respectively (*Figure 1(b)*). *Figure 2(a)* shows a typical sensor installation on the girder while *Figure 2(b)* shows the mid-span composite cross section of an interior girder with key dimensions and strain gage position illustrated. The sampling frequency of the strain gages is set at 100 Hz. The NRB monitoring system collects data from the *Narada* nodes using a base station computer which communicates data to the Internet via a cellular modem.

2.2 Cyber-Physical System (CPS) Design

Besides the NRB bridge monitoring system, the I-275 corridor has other data collecting elements within the CPS architecture including three traffic cameras and a WIM station (*Figure 3*). The WIM station is located 7 miles (11.3 km) north of the NRB and is managed by MDOT. It is a two-lane type II quartz station that measures vehicle gross weight, speed, number of axles, axle spacing, and axle weights. Each traffic camera is a Logitech C930e webcam controlled by a GPU-enabled embedded computing device (Nvidia Jetson TX2) which is connected to the Internet through a cellular modem. Each camera is programmed to capture traffic images at a frame rate of 10 FPS

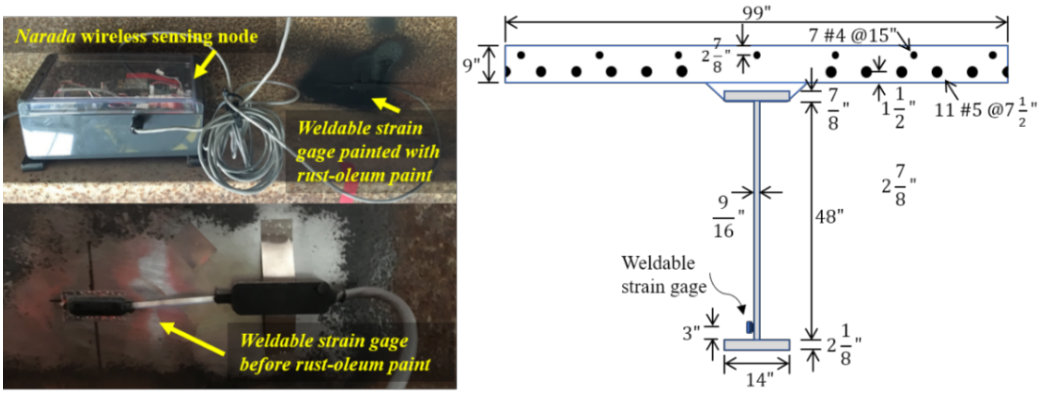

Figure 2. (left) Strain gage installation on the Newburg Road Bridge; (right) cross section of an interior girder with dimension and sensor location illustrated.

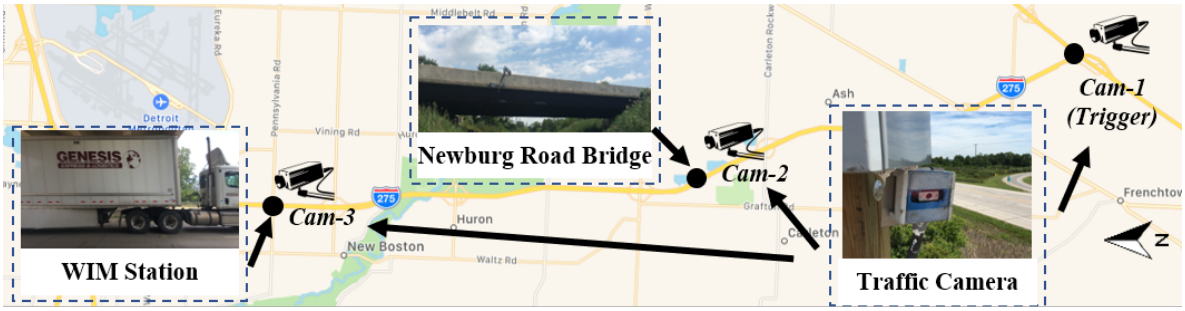

Figure 3. Locations of the cyber-physical system components along the I-275 north bound corridor.

with a resolution of 1280x720 pixels. A vehicle detection program, namely YOLOv3-tiny (Redmon and Farhadi 2018), is embedded in each TX2 for real-time truck detection using captured images. Cam-1 (*Figure 3*) is 6.5 miles (10.5 km) upstream from the NRB acting as a trigger of the entire CPS architecture. Cam-2 and Cam-3 are installed at the NRB and WIM station to capture truck images synchronized with bridge response data and truck weight data, respectively. Bridge response data, WIMS truck weight data and the corresponding truck images (taken from Cam-1, Cam-2, and Cam-3) are communicated to a cloud-based data management system developed for data storage and computing (Jeong et al. 2018).

After a truck is detected by Cam-1, it messages the other downstream CPS elements (Cam-2, Cam-3 and the NRB monitoring system) via the Internet to begin their data acquisition processes starting at a time based on the approximate travel time of the truck. The NRB bridge monitoring system and Cam-2 are programmed to collect data for 120 seconds with a delay of 300 seconds (corresponding to 6.5-mile driving distance at 65 mph) after a positive detection of a truck at Cam-1. By the same logic, Cam-3 collects images for 200 seconds with a delay of 630 seconds from detection at Cam-1. Operated by MDOT, the WIM station is collecting data at all times and communicating it to a WIMS database that the CPS architecture has access to. Following this coordinated data collection process, the CPS architecture is capable of tracking the same truck along the instrumented highway corridor.

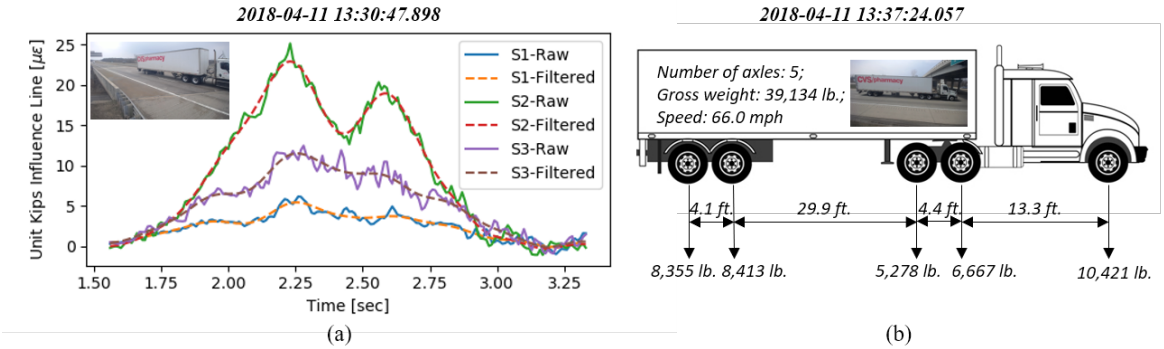

Figure 4. Paired weigh-in-motion and structural monitoring data: (a) time history of bridge strain responses measured by strain gages S1, S2 and S3 with a picture of the truck; (b) measured weight configuration at the WIM station with a picture of the same truck.

All data collected (i.e., bridge strains, camera frames, and WIM record) within the same data collection cycle are automatically uploaded to a server hosted in the cloud. When uploading is completed, a program on the CPS sever automatically detects and synchronizes truck events between the different types of data at each location (i.e., the NRB and the WIM station), after which each detected truck event is segmented from the original data set as a set of truck images plus either the bridge monitoring data *(Figure 4(a)*) or truck weight data (*Figure 4(b)*). The truck images are key to linking the bridge responses to the WIM recording of the same truck. To re-identify the truck at the NRB and the WIM station, a learning-based re-identification algorithm is adopted to match the trucks (Hou et al. 2019). This is critical because the gross vehicle weight and the axle weight distributions for the truck can be used to interpret the strain response of the bridge. This provides an input-output data set similar to what would be obtained in a traditional field load test. However, the CPS approach does not require any interruption in traffic and has the potential to collect a large number of truck events. A sample of paired data corresponding to a 5-axle truck is shown in *Figure 4*. Totally, 6092 matched data pairs collected from November 2017 to September 2018 are utilized in this study to demonstrate the proposed data-driven load rating method. While only a single truck travels on the bridge at the same time in this data set, there could be the presence of small vehicles (e.g., cars) in a few of the data sets.

3. Data-Driven Load Rating Procedure

3.1 General Load Rating Equation and Items

This paper showcases the proposed data-driven load rating method by performing a design load rating following the LRFR method presented in the MBE (AASHTO 2018). The legal load rating and the permit load rating can be performed in a similar manner. According to the latest MBE, the general load rating equation for each component subjected to a single force effect (i.e., flexure) can be expressed as follows (AASHTO 2018),

$$RF = \frac{C - (\gamma_{DC})(DC) - (\gamma_{DW})(DW) \pm (\gamma_P)(P)}{(\gamma_{LL})(LL + IM)} \quad (1)$$

where *RF* is the rating factor of a structural component, *C* is its capacity given its current condition, *DC* is the dead load effect due to structural components and attachments, *DW* is the dead load effects due to wearing surface and utilities, *P* is permanent load effects other than those from the dead loads, *LL* is the live load effect, and *IM* represents additional live load effects produced by DLA. All of the γ-values are scaling load factors defined in the Load and Resistance Factor Design (LRFD) bridge design specifications (AASHTO 2017). All capacity and load effects are presented herein with respect to strain responses presented in micro-strain. As the structural components to be rated in this paper are three interior steel girders, the capacity of the girder is calculated based on the nominal resistance, *R*, of the girder cross section (*Figure 2(b)*) at the sensing location under flexural moment and scaled by LRFD factors (e.g., condition, system and resistance factors) (AASHTO 2018). The values of *DC, DW* and *P* are determined as per the bridge design drawings and a calibrated finite element model which is discussed in Section 3.2. The three dead load factors (γ_{DC}, γ_{DW}, γ_P) are determined according to the LRFD specifications. As both inventory-and operating-level ratings under the Strength I limit state are reported, the live load factor, γ_{LL}, has two values: 1.75 and 1.35 for the inventory- and operating-levels, respectively (AASHTO 2018).

In this paper, the HL-93 design live load is used for the design load rating with all combinations of different load scenarios (e.g., single-lane and multiple-lane loads) explicitly considered to generate the maximum live load effect (AASHTO 2017). The major contribution of this paper is on how to efficiently compute an accurate live load effect considering both the systematic behavior of the bridge and the current condition of its structural elements. This objective is achieved by extracting UILs and DLA from the multi-source data set collected by the instrumented CPS. The data processing procedures for extracting the DLAs and UILs are discussed in Sections 3.3 and 3.4, respectively.

3.2 Finite Element Modelling

A finite element model of the NRB is created in the commercial FEM package CSiBridge 2016 using the engineering drawings and materials test results of the bridge. The concrete deck and steel girders are modelled using shell elements while the bridge bracings and stiffeners are modelled using frame elements. The reinforcement effect of the slab reinforcement bars on the deck stiffness is included by setting a deck stiffness amplification factor in CSiBridge. Bridge boundary conditions are modelled using translational and rotational springs. The model is calibrated by tuning the coefficients of these boundary springs by matching modal features (e.g., modal frequencies) of the model with those extracted from the monitoring data and based on minimizing the difference between predicted and measured strains under truck loading. The CSiBridge model is also used for computing all dead load effects.

3.3 Dynamic Load Allowance

DLA is in effect an amplification of the live load effect induced by moving vehicle wheel loads as compared to static wheel loads. The DLA value recommended by the MBE for steel girders in the load rating cases considered in this paper is 33%. (AASHTO 2018). It has been widely studied that the DLA of a bridge is strongly influence by many factors including the type of bridge and its geometry. Also influencing the DLA are the vehicle properties including its speed, weight and

suspension system (Deng et al. 2015b; a; Paultre et al. 1992). This results in a high variation in the DLA for a specific bridge (Carey et al. 2017). In this study, DLA is extracted from the measured vehicle weight and bridge response data based on the use of low-pass filtering of the measured bridge strain (Paultre et al. 1992). The filter needs a cut-off frequency lower than the bridge's first natural frequency and a passband of *v/L* Hz, where *v* is the speed of passing vehicles and *L* is the bridge span length. The NRB exhibits its first mode at 4.2 Hz; the vehicle passing frequency can range from 0.77 Hz to 1.11 Hz assuming vehicle speed ranging from 55 mph to 80 mph, respectively. Consequently, a low-pass filter with a 3.5 Hz cut-off frequency is used to filter the measured dynamic strain response to derive the bridge static responses. *Figure 4(a)* overlaps the measured raw data with the low-pass filtered data to illustrate the process. The DLA can then be calculated as follows,

$$DLA = \frac{max\ (R_{dyn} - R_{sta})}{max\ (R_{sta})} \tag{2}$$

where R_{dyn} is the dynamic response and R_{sta} is the static (i.e., low-pass filtered) response.

The scatter plots of extracted DLA values versus vehicle gross weight under different loading scenarios are shown in *Figure 5*. As labelled in *Figure 5,* each subplot corresponds to a girder sensor location (S1, S2 or S3) and a truck lane assignment (slow, middle or fast lane). It should be noted that the number of samples corresponding to trucks in the fast lane is small as few trucks choose to use the fast lane when crossing the bridge. As can be seen, the extracted DLA values vary widely with generally more variation at lower vehicle weights. This is expected as lower weight vehicles induce a smaller static strain response leading to the DLA calculation being strongly influenced by signal noise. Hence, the DLA extraction process focuses on DCA values that correspond to truck weights corresponding to the dominating HL-93 load pattern. For the NCB, the dominant HL-93 load pattern corresponds to an HS-20 truck with the uniform design lane load. The gross weight of the HS-20 design truck, 72 kips, is notated using a vertical solid green line in each subplot. A region of interest (ROI) is established around 72 kips to account for the maximum 15% error of the WIM station in terms of vehicle gross weight. All samples within this region are considered for the extraction of DLA values for the HS-20 design truck load. The mean, μ, and standard deviation, σ, of all the DCA samples in the ROI are calculated, and the estimated DLA (shown as the solid black horizontal line in *Figure 5*) is taken as $\mu+3\sigma$ to screen out extreme values (outliers) which might be caused by either sensor noise or a faulty WIM measurement. The MBE recommended DLA value (0.33) is presented as the red dashed line in each subplot for reference. It can be observed that the DLA values tend to be smaller for heavier trucks. The relative position of the truck relative to the girder line is important. Specifically, the DLA value of a girder tends to be smaller (usually below 0.33) when the vehicular loads are on the lane right above the girder and a larger portion of the vehicular load is distributed to it. For example, the DLA value of S1 is smaller when the truck is assigned to the slow lane. This can be due to the load distribution in the bridge section with the girder closest to the truck lane taking a larger share of the live load response leading to improved signal-to-noise ratios. Taking the DLA for the loads above the sensor, the data suggests the MBE over estimates the DLA value for a bridge like the NRB. The obtained DLA values are used to compute the worst loading scenario with the HL-93 design load.

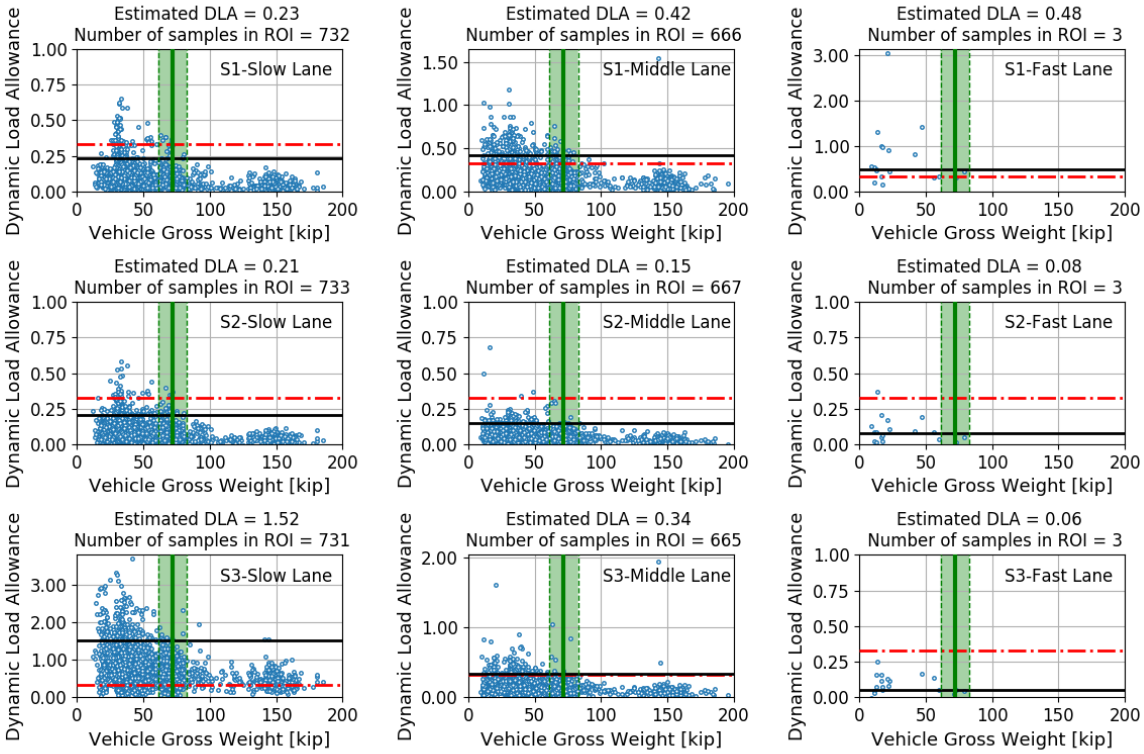

Figure 5. Dynamic load allowance (DLA) values extracted from NCB strain data under different loading scenarios (truck in slow, middle of fast lane) for the three sensing locations (S1, S2, and S3). Solid vertical green line corresponds to 72-kip HS-20 load, shaded green region is the region of interest (ROI), red horizontal line corresponds to the AASHTO DLA (0.33) and the black line is the $\mu+3\sigma$ DLA for samples in the ROI.

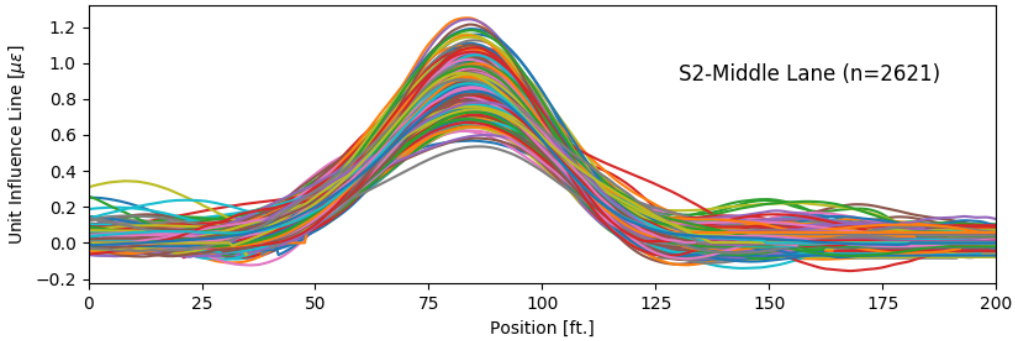

Figure 6. Extracted unit influence lines for sensor S2 when trucks travel along the NCB middle lane.

3.4 Unit Influence Line

A UIL represents the load effect (defined here using strain) induced at a specific bridge location caused by a unit axle load (one kip) traversing the bridge over a defined certain lane. While being continuous in theory, the lane positions along the bridge length are usually discretized so that the UIL can be conveniently expressed as a vector. For each pair of measured bridge strain and truck load configuration (particularly axle spacings and weights), a unit load influence line can be extracted at each sensor location by solving a series of linear equations formulated based on

fundamental input-output relations of *Equation (3)* where ε_t is the strain measurement at timestamp t, w_i is the i^{th} axle weight at timestamp t, and I_{it} is the UIL entry corresponding to the position of i^{th} axle at timestamp t that is being solved for (O'Brien et al. 2006):

$$\varepsilon_t = \sum_{i}^{N} w_i I_{it} \tag{3}$$

The algorithm proposed by O'Brien et al. (2006) is used to extract I_{it}. The static (low-pass filtered) strain responses are used as the input strain for the extraction of the UIL. With over 6,000 bridge-truck data sets available for this study, thousands of influence lines can be extracted for each sensing location and truck lane assignment. Like the DLA extraction case, there will be fewer UILs for the case of trucks assigned to the fast lane. Considering that the sampling frequency of the strain gage is 100 Hz and the truck speed limit is 65 mph along the I-275 corridor, the UILs is discretized with a resolution of 11.4 inches (28.9 cm). While the UIL is supposed to be a 105-entry vector given the proposed discretization, the obtained UIL vectors are larger since it is impossible to determine the exact timestamps when trucks enter and exit the bridge and redundant tiny entries are added to the head and tail of calculated UILs (O'Brien et al. 2006). Those values are very close to zero and thus won't influence of the final predicted responses. The entries at the tail are usually larger than those at the head due to free vibration after trucks leave the bridge.

A total of 2621 UILs are extracted for S2 when the axle load is moving on the middle lane as plotted in *Figure 6*. It can be observed that the extracted influence lines have similar shapes but vary in amplitude. This variation can be attributed to many factors such as varying truck speeds, varying truck location within the lane, different load configurations of the trucks, WIM data error, bridge response error, presence of small vehicles, and signal noise. In this study, the magnitude of the final UIL is selected to be the mean value at each position. The final extracted UIL for all three sensors with different loading lanes are plotted in *Figure 7*. They are used to generate the maximum vehicular live load effect combined with the extracted DLA values.

4. Load Rating Evaluation

Given the extracted DLA values and UIL vectors under different loading scenarios, the maximum live load effect caused by the HL-93 design load can be calculated for all three girders. The results are listed in *Table 1* along with results obtained from the FEM simulations in CSiBridge. It can be observed that both methods obtain the maximum live load effect under the same load conditions. The results by the data-driven method are higher than that from FEM. To evaluate the proposed data-driven load rating method, the resultant rating factors are compared with those obtained by the FEM-based method in *Table 2*. Included is the conventional analytical method following the logic of *Equation (1)*. The results, as listed in *Table 2*, show that the rating factors calculated using the data-driven approach lie between the conventional and the FEM-based rating factors.

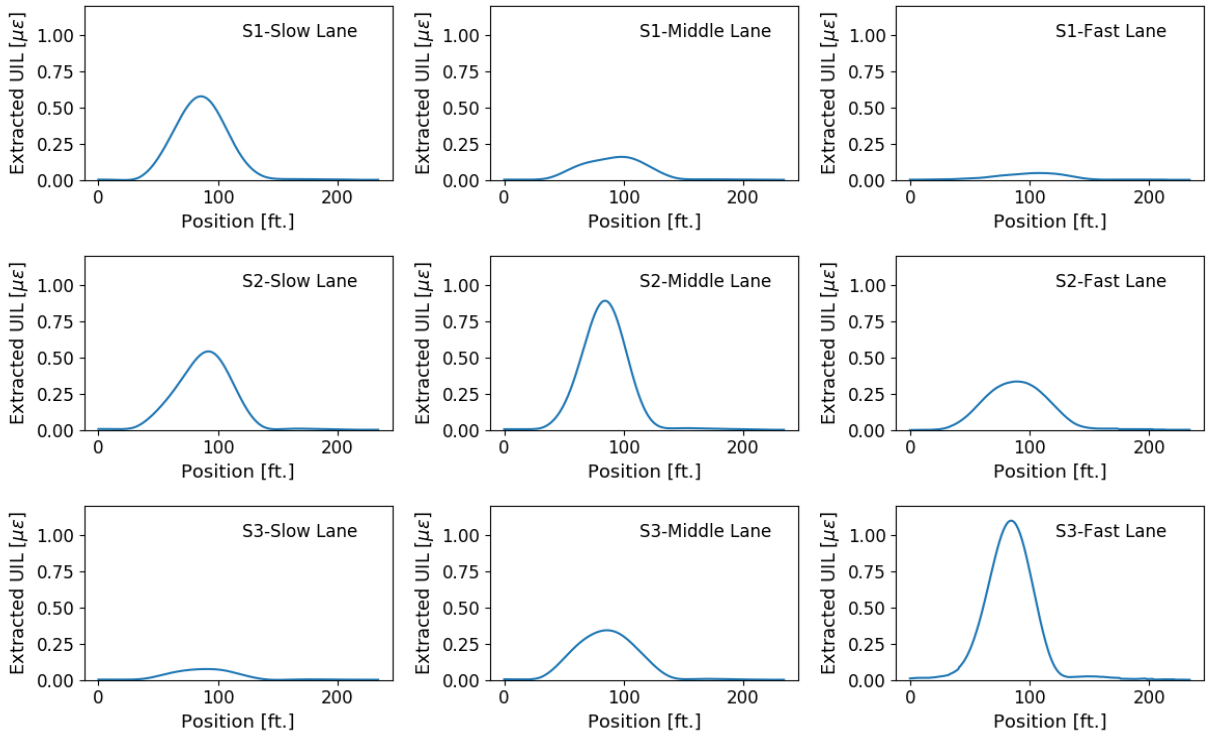

Figure 7. Unit influence lines (UIL) extracted for the NRB three sensing locations with different loading lanes.

Table 1. Maximum live load effects computed using the proposed data-driven method and the FEM-based method

	Girder 2 (S1)	Girder 4 (S2)	Girder 6 (S3)
Live Load Effect (Data-driven Method)	88.97 $\mu\varepsilon$	164.26 $\mu\varepsilon$	152.34 $\mu\varepsilon$
Live Load Effect (FEM-based Method)	78.88 $\mu\varepsilon$	134.87 $\mu\varepsilon$	108.55 $\mu\varepsilon$
Worst Load Case	HL-93 load on slow and middle lane	HL-93 load on slow, middle and fast lane	HL-93 load on middle and fast lane

Table 2. Load rating factors calculated by three different methods

		Girder 2 (S1)	Girder 4 (S2)	Girder 6 (S3)
Inventory Level Rating Factor	Conventional	1.45	1.45	1.45
	FEM-based	4.66	2.66	3.42
	Data-driven	4.14	2.17	2.34
Operating Level Rating Factor	Conventional	1.88	1.88	1.88
	FEM-based	6.05	3.43	4.43
	Data-driven	5.19	2.81	3.03

5. Conclusions

Accurate load ratings are critical for effective bridge management. In this study, a cyber-physical system that consists of bridge health monitoring system, cameras and a WIM are integrated within

a single CPS architecture to collect and integrate bridge and truck measurement data. By doing so, a vast collection of bridge response data paired with vehicular weight data can be collected at minimal cost and effort. Taking advantage of the data, realistic parameters under different loading conditions such as dynamic load allowance and unit influence lines can be calculated to produce a more accurate data-driven rating factor reflecting the bridge's actual load-carrying capacity. Future research will focus on investigating the factors that influence the quality of the extracted UILs and testing the generalizability of the proposed method on another multiple-span bridge located on the same highway corridor.

Acknowledgments

This work was supported by the National Science Foundation (NSF) (Grants ECCS-1446521 and ECCS-1446330). Any opinions, findings, and conclusions or recommendations expressed in this paper are those of the authors and do not necessarily reflect the views of NSF. Additional in-kind support was provided by the Michigan Department of Transportation (MDOT) including MDOT personnel providing on-site installation assistance; this assistance is gratefully acknowledged.

References

AASHTO. (2017). *AASHTO LRFD bridge design specifications (8th edition)*. American Association of State Highway and Transportation Officials (AASHTO), Washington, DC.

AASHTO. (2018). *Manual for bridge evaluation (3rd edition)*. Washington, DC.

Al-Khateeb, H. T., Shenton, H. W., and Chajes, M. J. (2018). "Computing continuous load rating factors for bridges using structural health monitoring data." *Journal of Civil Structural Health Monitoring*, Springer, 8(5), 721–735.

Alipour, M., Harris, D. K., and Ozbulut, O. E. (2016). "Vibration testing for bridge load rating." *Dynamics of Civil Structures, Volume 2*, Springer, 175–184.

Bell, E. S., Lefebvre, P. J., Sanayei, M., Brenner, B., Sipple, J. D., and Peddle, J. (2013). "Objective load rating of a steel-girder bridge using structural modeling and health monitoring." *Journal of Structural Engineering*, American Society of Civil Engineers, Reston, VA, 139(10), 1771–1779.

Carey, C., O'Brien, E. J., Malekjafarian, A., Lydon, M., and Taylor, S. (2017). "Direct field measurement of the dynamic amplification in a bridge." *Mechanical Systems and Signal Processing*, Elsevier, 85, 601–609.

Catbas, F. N., Zaurin, R., Gul, M., and Gokce, H. B. (2012). "Sensor networks, computer imaging, and unit influence lines for structural health monitoring: case study for bridge load rating." *Journal of Bridge Engineering*, 17(4), 662–670.

Deng, L., He, W., and Shao, Y. (2015a). "Dynamic impact factors for shear and bending moment of simply supported and continuous concrete girder bridges." *Journal of Bridge Engineering*, American Society of Civil Engineers, Reston, VA, 20(11), 4015005.

Deng, L., Yu, Y., Zou, Q., and Cai, C. (2015b). "state-of-the-art review of dynamic impact factors of highway bridges." *Journal of Bridge Engineering*, 20(Im), 1–14.

Deng, Y., and Phares, B. M. (2016). "Automated bridge load rating determination utilizing strain response due to ambient traffic trucks." *Engineering Structures*, Elsevier, 117, 101–117.

Hou, R., Jeong, S., Lynch, J. P., and Law, K. H. (2019). "Reidentification of truck loads in

highway corridors using convolutional neural networks to link measured truck weights to bridge responses." *SPIE Smart Structures + Nondestructive Evaluation 2019*.

Hou, R., Jeong, S., Wang, Y., Law, K. H., and Lynch, J. P. (2017). "Camera-based triggering of bridge structure health monitoring systems using a cyber-physical system framework." *International Workshop on Structural Health Monitoring 2017 (IWSHM 2017)*.

Jeong, S., Hou, R., Lynch, J. P., Sohn, H., and Law, K. H. (2018). "A scalable cloud-based cyberinfrastructure platform for bridge monitoring." *Structure and Infrastructure Engineering*, Taylor & Francis, 0(0), 1–21.

Ndong, A. K., Dizaji, M. S., Alipour, M., Ozbulut, O. E., and Harris, D. K. (2019). "Load rating of a reinforced concrete T-beam bridge through ambient vibration testing and finite element model updating." *Dynamics of Civil Structures, Volume 2*, Springer, 337–343.

O'Brien, E. J., Quilligan, M. J., and Karoumi, R. (2006). "Calculating an influence line from direct measurements." *Proceedings of the Institution of Civil Engineers - Bridge Engineering*, 159(1), 31–34.

Paultre, P., Chaallal, O., and Proulx, J. (1992). "Bridge dynamics and dynamic amplification factors—a review of analytical and experimental findings." *Canadian Journal of Civil Engineering*, NRC Research Press, 19(2), 260–278.

Redmon, J., and Farhadi, A. (2018). "YOLOv3: an incremental improvement."

Sanayei, M., Reiff, A. J., Brenner, B. R., and Imbaro, G. R. (2015). "Load rating of a fully instrumented bridge: comparison of LRFR approaches." *Journal of Performance of Constructed Facilities*, American Society of Civil Engineers, Reston, VA, 30(2), 4015019.